Desalination and Water Treatment
www.deswater.com
doi: 10.1080/19443994.2013.780994

51 (2013) 6338–6345
September

Taylor & Francis
Taylor & Francis Group

Novel thin nanocomposite RO membranes for chlorine resistance

Sang Gon Kim, Dong Hun Hyeon, Jeong Hwan Chun, Byung-Hee Chun, Sung Hyun Kim*

Department of Chemical & Biological Engineering, Korea University, 1 Anam-Dong, Seongbuk-Gu, Seoul 136-701, Korea
Tel. +82 2 3290 3297; Fax: +82 2 926 6102; email: kimsh@korea.ac.kr

Received 28 November 2012; Accepted 28 January 2013

ABSTRACT

Sulfonated poly(arylene ether sulfone) material containing amino groups (aPES) is successfully synthesized using aromatic substitution polymerization. This material was shown to be a novel thin-film composite (TFC) reverse osmosis (RO) membrane material with high chlorine resistance. Graphene oxide (GO) and aminated graphene oxide (aGO) nanoparticles were also prepared. TFC membranes were prepared using an interfacial polymerization (IP) reaction with trimesoyl chloride (TMC) and amine solution, containing synthesized materials, on a polysulfone (PS) ultrafiltration (UF) support membrane. The synthesized aPES and fabricated TFC RO membranes were characterized by nuclear magnetic resonance spectroscopy and scanning electron microscope. Moreover, RO performances, salt rejection, and water flux were measured using cross-flow cell instrument. The chlorine resistance was evaluated using sodium hypochlorite solution. The membrane fabricated with aPES/GO/aGO was compared with the typical polyamide (PA) TFC membrane which was prepared by the IP reaction with TMC and MPDA on a PS support membrane. The aPES/GO/aGO RO membrane had much higher chlorine resistance than PA RO membrane and showed good RO performances, such as water flux (28 $L/m^2 h$) and salt rejection (98%).

Keywords: Desalination; Reverse osmosis; RO membrane; Sulfonated poly(arylene ether sulfone); Chlorine-resistance

1. Introduction

Reverse osmosis (RO) is the most widely used desalination technology worldwide. RO has overtaken conventional thermal technologies such as multi-stage flash [1], and the widespread use is expected to continue despite advances in other technologies, such as membrane distillation [2], electrodialysis [3], and forward-osmosis [4]. Commercial interest in RO technology is increasing globally because of continuous process improvements, which in turn lead to significant cost reductions. These advances include developments in membrane materials, process design, feed pre-treatment, and energy recovery or reduction in energy consumption [5, 6].

Over the past few decades, remarkable advances have been made in the preparation of RO membranes

*Corresponding author.

Presented at The Fifth Desalination Workshop (IDW 2012), October 28–31, 2012, Jeju, Korea

from different materials. However, reviews on RO membrane materials are rare, likely because RO membrane design of practical importance is patented rather than examined through conventional academic research.

The published comprehensive review on RO membrane materials was by Petersen more than 17 years ago. This review focused only on the thin-film composite (TFC) membranes in existence at that time. Recently, Li and Wang published a review of research on RO membrane surface modification. In addition to ongoing research towards the development of conventional polymeric RO membrane materials, nanotechnology incorporates the use of nanomaterials into RO processes. It is therefore time to review the historical development of commercially successful RO membrane materials comprehensively, and to discuss novel nanostructured materials that will shape the future trends in the research of membrane materials.

Various chemicals have been tried to produce the active layer, such as poly(vinyl alcohol), polybenzimidazole, polyether, etc. The cross-linked aromatic polyamide (PA) which is produced via interfacial polymerization of m-phenylenediamine (MPDA) and trimesoyl chloride (TMC) has been used for commercial seawater desalination membranes [7,8]. The polyamide TFC membrane has a very high salt separation performance and good mechanical strength, and the performance of the PA TFC membrane has improved over the last 40 years. However, the main weakness of the PA TFC membranes is that free chlorine in the seawater attacks the active layer of PA and degrades the amide bond of the active layer [9].

Many materials and methods have been developed to overcome the weakness of PA TFC membranes. Among these polymers, sulfonated poly(arylene ether sulfone) (PES) materials are of considerable interest because these materials have good mechanical properties, and high chemical and thermal stability. Sulfonated poly(arylene ether sulfone)s do not contain the vulnerable amide bone that is susceptible to chlorine attack. More recently, some studies have prepared and characterized poly(arylene ether sulfone) materials [10–16].

Nanocomposite membrane technology has produced several new classes of materials for seawater desalination and water purification. Functional proper nanoparticles in a membrane matrix might enhance the mechanical and chemical stability as well as separation performances [17,18].

In this study, we prepared sulfonated poly(arylene ether sulfone) material containing amino groups (aPES). In addition, we prepared nanocomposite membranes via layer-by-layer (LbL) assembly method based on solution dipping process and IP method. LbL assembly method is quite useful for preparing nanocomposite membrane and thickness control [19–22].

2. Methods

2.1. Materials

4,4′-Dichlorodiphenyl sulfone (DCDPS), m-aminophenol,anhydrous potassium carbonate (K_2CO_3), and graphite powder (particle size,<0.2 mm) were obtained from Aldrich. DCDPS and m-aminophenol were dried under vacuum at 80°C for 12 h for further purification. Anhydrous potassium carbonate was used as received. 3,3′-disulfonated-4,4′-dichlorodiphenyl sulfone (SDCDPS) was synthesized according to previously published methods [23] and dried under vacuum at 100°C for 24 h before use. Graphene oxide (GO) was prepared according to the Brodie method [24]. N,N-dimethylacetamide (DMAc), MPDA, ethylenediamine, TMC (Sigma-Aldrich), toluene, ethanol (J.T. Baker) and sulfuric acid (Daejung reagents and chemical) were used as received.

2.2. Synthesis of sulfonated poly(arylene ether sulfone) material containing amino groups

First, into a three-necked round-bottomed flask (250 ml) equipped with a mechanical stirrer, a N_2 inlet-outlet, and a Dean-Stark trap, m-aminophenol (6.66 g, 60 mmol) and K_2CO_3 (9.26 g, 66 mmol) were charged along with DMAc (90 ml) as a solvent and toluene (36.0 ml) as a azeotropic agent. The reaction mixture was stirred by refluxing at 150°C for 7 h, while toluene azeotropically removed water. Finally, the azeotropic solvent was completely removed after 7 h, and then SDCDPS (15.0 g, 30 mmol) was added into the reaction flask along with more DMAc (20 ml) and the reaction mixture was stirred by heating at 165°C for 24 h. The reaction solution was cooled to room temperature and diluted using DMAc. The solution was filtrated to remove inorganic salts and unreacted chemicals. After filtration, the product was isolated by precipitation in ethanol solution resulting in solid. The precipitated material was successively washed several times with ethanol and dried under vacuum at 90°C for 24 h.

2.3. Synthesis of aminated graphene oxide nanoparticles

The following experimental processes were used to synthesize aminated graphene oxide (aGO). A mixture of graphene oxide (1.0 g) and ethylenediamine (20 mL) was stirred at room temperature for 12 h under a N_2

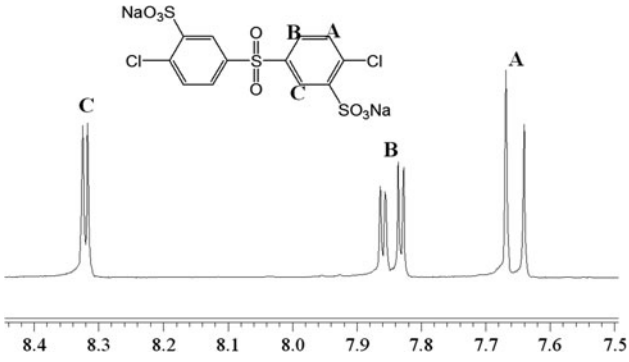

Fig 1. ^{1}H NMR spectroscopy result for SDCDPS in DMSO-d_6.

atmosphere. Next, the modified nanoparticles were filtered and thoroughly washed with deionized water, filtered, and dried at 80°C.

2.4. Fabrication of TFC reverse osmosis membrane

The method used for the formation of the PA TFC RO membrane is as follows. The polysulfone UF membrane was placed in an aqueous solution of 1% (w/v) MPDA for 2 min, and then rolled with a roller to remove excess solution of the membrane surface. Then, the membrane was immersed into a solution of 1% (w/v) TMC in cyclohexane for 1 min. After removing the excess solution, the membrane was heated in an oven at 70°C for 1 min for further polymerization.

aPES membrane was prepared according to the method as follows: The polysulfone UF membrane was placed in the aqueous solution containing a 1% (w/v) mixture of aPES and MPDA, triethylamine, (1%) and dodecyl sulfonic acid sodium salt (0.05%). The solution was then rolled with a roller to get rid of excess solution of the membrane surface. The membrane was immersed into a solution of 1% (w/v) TMC in cyclohexane for 5 min. After removing the solution, the membrane was treated in an oven at 70°C for 1 min.

aPES/GO/aGO nanocomposite membrane was prepared as follows: The solution concentration of GO and aGO was adjusted to 1 mg mL^{-1}. The pH of the GO and aGO solutions was controlled by 0.1 M HCl and NaOH without the addition of ionic salts. For the deposition of LbL assembled multilayer films onto the PS support layer, negatively charged PS substrates were prepared by a treatment with a H_2SO_4 solution at 80°C for 30 min. The PS support layer was first dipped in the cationic aGO solution for 10 min, washed twice in deionized water for 1 min each, and air-dried with a gentle stream of N_2. The anionic GO was then deposited onto the cationic aGO-coated substrates by adsorption for 10 min, washed in deionized water, and dried. This process was repeated until the desired number of layers had been deposited. To impose the chemical cross-linking between GO and aGO layers, the $(GO/aGO)_{15}$ multilayer membranes were heated at 180°C for 1 h under vacuum condition. After this LbL process, MPDA-TMC PA active layer was formed via IP method described above.

2.5. Characterization

The aPES was identified by elemental analysis, such as C, H, H. ^{1}H NMR spectra of the products were obtained at 300 MHz on the Varian Mercury 300 spectrometer using dimethyl sulfoxied-d_6 (DMSO-d_6) as a solvent. Fourier transform-infrared (FT-IR) characterization was accomplished using a Bomen DA-8 spectrometer. Hydrophilicity of the membrane surface was assessed by measuring the contact angle of water droplets with an Automatic Contact Angle Analyzer (Phoenix 300; Surface Electro Optics, Gyunggido, Korea). The membrane was imaged by scanning electron microscopy (SEM) with S-4300, Hitachi, Japan.

Membrane separation performance of the tested TFC RO membranes was tested with 32,000 ppm NaCl solution using the cross-flow cell apparatus and evaluated in terms of salt rejection and water flux. The effective membrane area was around 12.56 cm^2. All tests were conducted at room temperature at an applied pressure of 55 bars. Especially for the measurement of chlorine resistance, the membrane was immersed in aqueous sodium hypochlorite (NaOCl) solution (300 ppm).

3. Results and discussion

3.1. Characterization

SDCDPS was prepared via electrophilic aromatic substitution with DCDPS and sulfuric acid. The synthesis sequence of SDCDPS is outlined in Scheme 1.

The chemical composition and structure of SDCDPS were confirmed using elemental analysis and ^{1}H NMR spectroscopy with DMSO-d_6 as the solvent. The spectrum of SDCDPS is shown in Fig. 1. Assignment of each proton is shown in this figure, and these assignments agree with those of the proposed molecular structures of SDCDPS.

Sulfonated poly(arylene ether sulfone) containing amino groups was synthesized through polycondensation of 3,3′-disulfonated-4,4′-dichlorodiphenyl sulfone (aPES) and m-aminophenol in the presence of anhy-

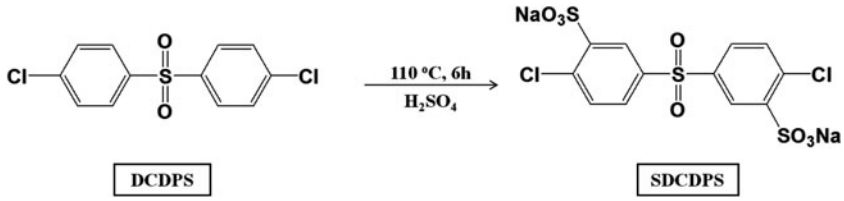

Scheme 1. The synthesis sequence of SDCDPS.

drous potassium carbonate in DMAc. Toluene was used as an azeotroping agent to remove water during the reaction. The reaction sequence of the sulfonated poly(arylene ether sulfone) sulfonic acid and amino groups is shown in Scheme 2.

^{1}H NMR was used to confirm the chemical structure of the copolymers and the spectrum of SDADPS with DMSO-d_6 as the solvent is shown in Fig. 2. Assignment of each proton is given in this figure and these agree with the proposed molecular structure of the sulfonated poly(arylene ether sulfone) containing sulfonic acid and amino groups.

The GO and aGO nanoparticles were successfully prepared using the Brodie method. FT-IR spectroscopy was used to identify the presence of related bonds, as shown in Fig. 3. Bands at 1,600 cm^{-1} and at 1,700 cm^{-1} indicate an ether bond and the presence of a carboxylate carbonyl group on GO and aGO spectra, respectively. For aGO spectra, bands at 1,100 cm^{-1} and 1,650 cm^{-1} were attributable to the presence of functional amine groups. These results verify that the GO and aGO nanoparticles were prepared successfully.

As shown in Fig. 4, the LbL multilayer of the $(GO/aGO)_{15}$ on the PS support membrane was successfully fabricated. The active layer surface of the TFC membranes were observed by SEM. Fig. 5 shows a SEM image of the polysulfone UF membrane surface and fabricated TFC RO membrane surface. As shown in Fig. 5, the surface of the TFC RO membrane exhibited the familiar "hill and valley" structure of PA RO membranes and the cross-section of TFC RO membrane indicated the presence of a thin, selective active layer, which was a few hundred nanometers thick, and was supported on a polysulfone UF support layer. The SEM images of the membrane confirmed that the TFC membrane was successfully fabricated.

AFM was used to investigate the surface morphology of the active layer overcoated onto the PS support layer. Fig. 6 shows the surface morphology of the composite membranes prepared using PA, aPES, and aPES/aGO. The bar at the bottom of each image indicates the vertical deviations in the sample; light regions indicate high deviation and dark regions indicate low deviation. Root-mean-square roughness (RMS) was defined as the mean of the root for the deviation from the standard surface to the indicated surface; and lower smaller RMS values indicate a smoother membrane surface. The RMS value of the aPES membrane (31 nm) was smaller than that of the PA membrane (55 nm) indicating a smoother surface on the aPES membrane than on the PA membrane. During interfacial condensation to form the thin-film

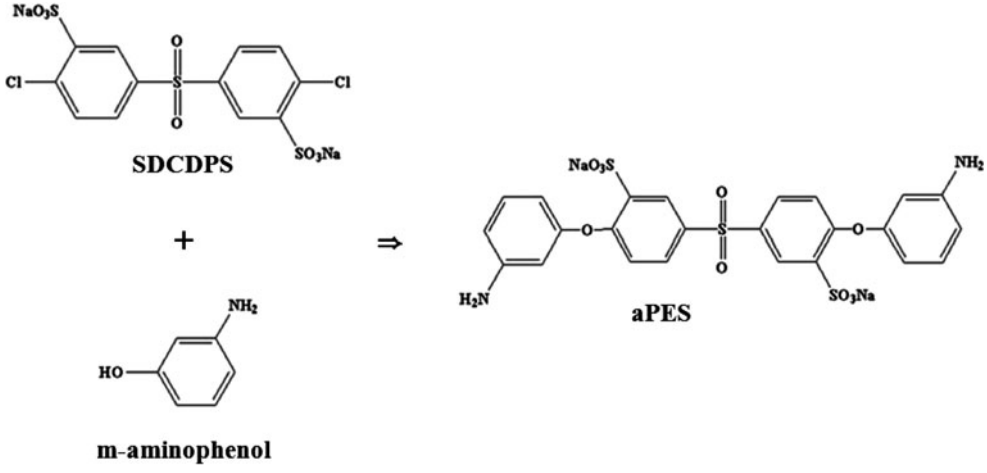

Scheme 2. The synthesis sequence of aPES.

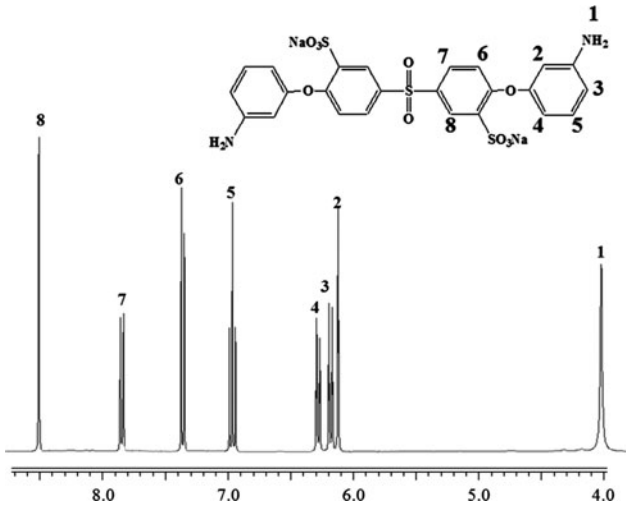

Fig 2. ^{1}H NMR spectroscopy of aPES.

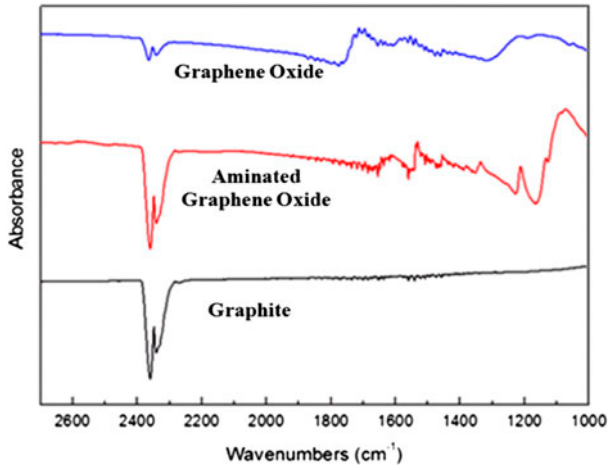

Fig 3. FT-IR spectra for graphite, GO, and aGO.

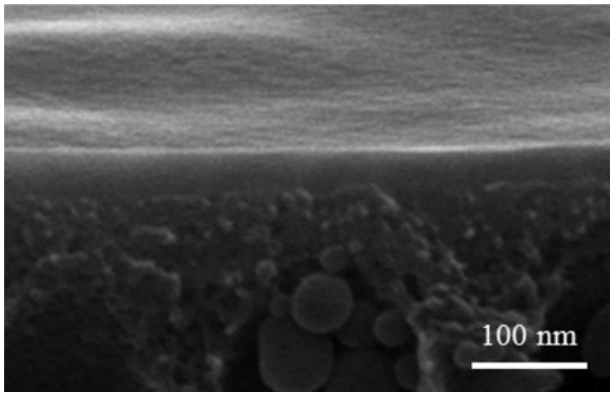

Fig 4. Cross-section SEM image of $(GO/aGO)_{15}$ multilayers prepared on PS support layer.

active layer, amine reactants dissolved in the aqueous phase diffused into the immiscible organic phase and reacted with TMC. Water-soluble polymeric amine reactants (aPES) are not expected to diffuse into the organic phase because of their poor solubility in the organic phase. As a result, cross-linking of PA and aPES would decrease the diffusion rate of amine reactants into the organic phase. Furthermore, the PA formed from MPDA and TMC involved grafting macromolecules onto aPES on the membrane surface, thus leading to smoother membrane-surface morphology.

3.2. Performances of RO membranes

The TFC RO membranes were fabricated by interfacial polymerization of the tri-functional biphenyl acid chloride (TMC) with a mixture of aPES and MPDA on the PS UF membrane. The RO performance of TFC membranes was evaluated with the cross-flow cell apparatus at 55 bar using a 32,000 ppm NaCl solution at room temperature. The RO performance of TFC membranes fabricated in this study was compared with that of the PA membrane produced in our laboratory. Fig. 7 shows the salt rejection and the water flux of the membranes.

The performance test showed that water flux was better in membranes containing aPES and a slight decrease in salt rejection was observed. The high performance of aPES membranes was due to the incorporation of the rigid and hydrophilic aPES material. Water flux of the membranes increased from 23.2 L/m^2 h (PA, prepared) to 32.5 L/m^2 h (aPES). As shown in Table 1, the contact angle data supported this increase in water flux. The contact angle decreased from 61.2° (PA) to 50.7° (aPES), explaining the increase in water flux. In addition, the aPES/GO/aGO membrane contained not only aPES material but also nanoparticles which may have produced additional amide bonds layer on the membrane. This resulted in improved salt rejection and decreased water flux in comparison with that of the aPES membrane.

The chlorine resistance test of the PA membrane showed that salt rejection decreased rapidly following chlorine exposure (98.0% to 67.2%), while salt rejection of the aPES membrane decreased slightly (94.3% to 75.6%). Water flux of the PA membrane increased significantly after chlorine solution treatment (23.2 L/m^2 h to 48.1 L/m^2 h), while water flux of the aPES membrane increased (28.4 L/m^2 h to 37.4 L/m^2 h). For the PA membrane, the decrease in salt rejection that accompanied the abrupt increase in flux of the PA membrane was due to chemical degradation of the amide bonds by free chlorine.

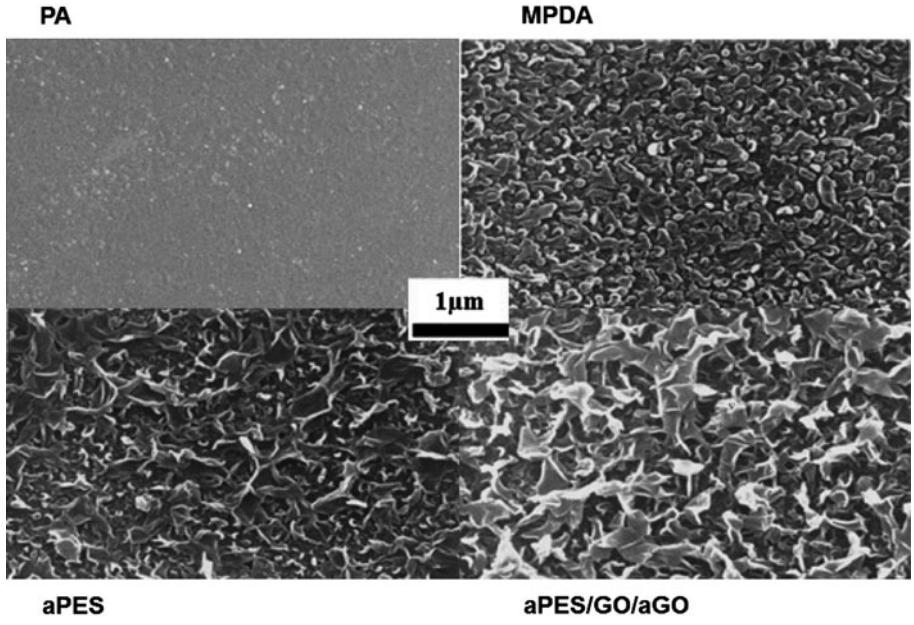

Fig 5. SEM images of membrane surfaces.

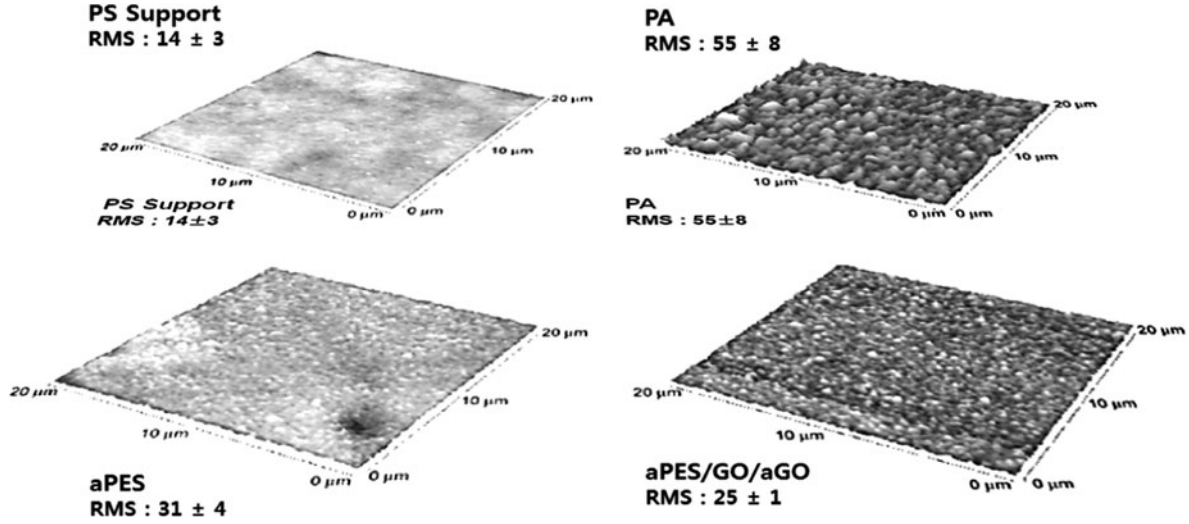

Fig 6. AFM surface images of the membranes.

When GO/aGO nanoparticles were introduced into the membrane matrix, the membranes displayed improved chlorine resistance. Salt rejection of the aPES/GO/aGO membrane decreased from 98.4% to 84.2%, while salt rejection of the aPES membrane decreased from 94.3% to 75.6%. The decreased salt rejection rate of the aPES/GO/aGO membrane was less than that of the aPES membrane. The increased water flux rate of the aPES/GO/aGO membrane (28.4 $L/m^2 h$ to 37.3 $L/m^2 h$) was less than that of the aPES membrane (32.5 $L/m^2 h$ to 45.7 $L/m^2 h$). Thus, the amide bonds were more protected when GO/aGO nanoparticles were introduced into the membrane. In membranes that contain nanoparticles, the intermolecular hydrogen bonding is enhanced by the bonding between the nanoparticles and the PA structure. This can be expected to impede the replacement of hydrogens on the amide groups of the aromatic PA membranes with chlorine. Furthermore, the amino groups on the GO/aGO combine to form amide bonds in the RO membrane active layer. These additional amide bonds and unreacted amino groups of the nanoparticle further protect the active layer from chlorine. Therefore, the addition of nanoparticles assists in

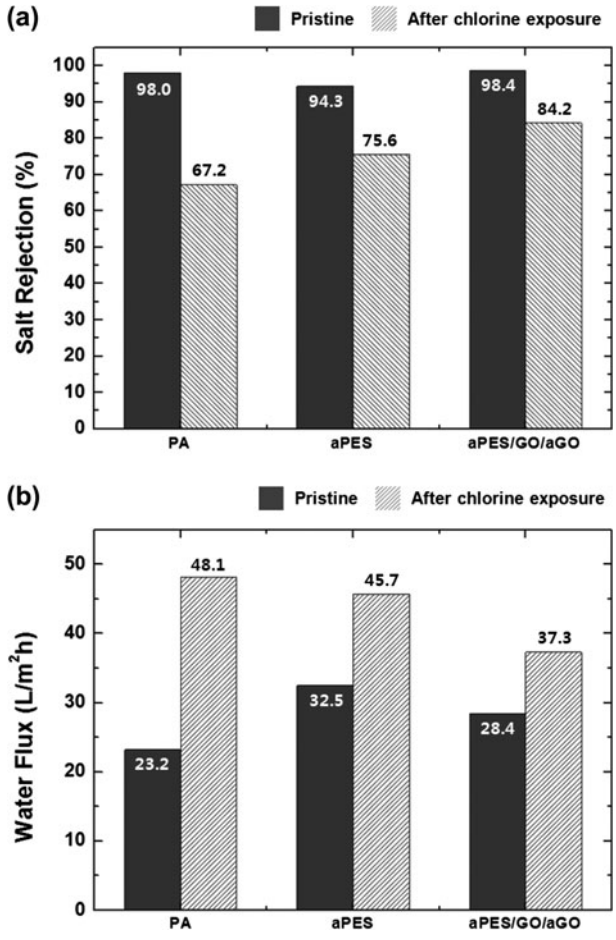

Fig 7. Comparison of the RO performances and chlorine resistance of the RO membranes; (a) salt rejection and (b) water flux.

Table 1
Contact angles of the membranes

Samples	Contact angle (°C)
PA	61.2
aPES	50.7
aPES/GO/aGO	55.4

protecting the PA structure from degradation through chlorination, and is effective in improving the hydrophilicity of the active layer of the TFC membrane.

4. Conclusions

Sulfonated poly(arylene ether sulfone) containing amino groups was successfully synthesized via an aromatic substitution reaction from SDCDPS and m-aminophenol in the presence of anhydrous potassium carbonate in DMAc; this was confirmed using ^{1}H NMR.

Three types of TFC RO membranes were successfully fabricated using the interfacial polymerization method on a polysulfone UF substrate. Chemical and physical structures were verified using FT-IR analysis and SEM images. All the membranes were prepared using the same technique.

The aPES/GO/aGO membrane displayed good chlorine resistance; its RO performance was comparable to that of the PA membrane. Water flux of the aPES/GO/aGO membrane was 28.4 L/m^2 h, which was higher than that of the PA membrane (23.2 L/m^2 h). In addition, the aPES/GO/aGO membrane showed a much higher chlorine resistance than the PA and aPES membrane. This was due to the presence of nanoparticle layer and hydrophilic sulfonated poly(arylene ether sulfone) material containing amino groups.

In conclusion, the aPES/GO/aGO RO membrane, which displayed a high chlorine resistance and good RO performance, shows promise for use in the seawater desalination process, without significant decrease in performance due to the presence of chlorine.

Acknowledgment

This research was supported by a grant (#12 seaHERO B02-06) from Plant Technology Advancement Program funded by the Ministry of Land, Transport and Maritime Affairs of the Korean government.

References

[1] J.E. Cadotte, US Patent 4,277,344 (1981).
[2] S.A. Sundet, US Patent 4,520,044 (1985).
[3] R.F. Fibiger, J.Y. Koo, D.J. Fogach, R.J. Petersen, D.L. Schmidt, R.A. Wessling, T.F. Stocker, US Patent 4,769,148 (1988).
[4] J.E. Tomaschke, US Patent 4,872,984 (1989).
[5] I.J. Roh, J.J. Kim, S.Y. Park, C.K. Kim, Effects of the polyamide molecular structure on the performance of reverse osmosis membranes, J. Polym. Sci. Part B 36 (1998) 1821–1830.
[6] C.K. Kim, J.H. Kim, I.J. Roh, J.J. Kim, The changes of membranes performance with polyamide molecular structure in the reverse osmosis process, J. Membr. Sci. 165 (2000) 189–199.
[7] J.E. Cadotte, R.J. Petersen, R.E. Larson, E.E. Erickson, New thin-film composite seawater reverse-osmosis membrane, Desalination 32 (1980) 25–31.
[8] G. Chen, S. Li, X. Zhang, S. Zhang, Novel thin-film composite membranes with improved water flux from sulfonated cardo poly(arylene ether sulfone) bearing pendant amino groups, J. Membr. Sci. 310 (2008) 102–109.
[9] P.R. Buch, D. Jagan Mohan, A.V.R. Reddy, Preparation, characterization and chlorine stability of aromatic-cycloaliphatic polyamide thin film composite membranes, J. Membr. Sci. 309 (2008) 36–44.
[10] D.S. Kim, K.H. Shin, H.B. Park, Y.S. Chung, S.Y. Nam, Y.M. Lee, Synthesis and characterization of sulfonated poly(arylene ether sulfone) copolymers containing carboxyl groups for direct methanol fuel cells, J. Membr. Sci. 278 (2008) 428–436.

[11] S.J. Im, R. Patel, S.J. Shin, J.H. Kim, B.R. Min, Sulfonated poly (arylene ether sulfone) membranes based on biphenol for direct methanol fuel cells, Korean J. Chem. Eng. 25 (2008) 732–737.
[12] M. Paul, H.B. Park, B.D. Freeman, A. Roy, J.E. McGrath, J.S. Riffle, Synthesis and crosslinking of partially disulfonated poly(arylene ether sulfone) random copolymers as candidates for chlorine resistant reverse osmosis membranes, Polymer 49 (2008) 2243–2252.
[13] K.T. Park, J.H. Chun, S.G. Kim, B.H. Chun, S.H. Kim, Synthesis and characterization of crosslinked sulfonated poly(arylene ether sulfone) membranes for high temperature PEMFC applications, Int. J. Hydrogen Energy 36 (2011) 1813–1819.
[14] H.S. Lee, A. Roy, O. Lane, S. Dunn, J.E. Mcgrath, Hydrophilicehydrophobic multiblock copolymers based on poly(arylene ether sulfone) via low-temperature coupling reactions for proton exchange membrane fuel cells, Polymer 49 (2008) 715–723.
[15] J.F. Blanco, Q.T. Nguyen, P. Schaetzel, Novel hydrophilic membrane materials: Sulfonated polyethersulfone Cardo, J. Membr. Sci. 186 (2001) 267–279.
[16] H.S. Lee, A.S. Badami, A. Roy, J.E. Mcgrath, Segmented Sulfonated Poly(arylene ether sulfone)-b-Polyimide Copolymers for Proton Exchange Membrane Fuel Cells. I. Copolymer Synthesis and undamental Properties, J. Polym. Sci. Part A 45 (2007) 4879–4890.
[17] W.J. Koros, Evolving beyond the thermal age of separation processes: Membrane can lead the way, AIChE Journal 50 (2004) 2326–2334.
[18] B.H. Joeng, E.M.V. Hoek, Y. Yan, A. Subramani, X. Huang, G. Hurwitz, A.K. Ghosh, A. Jawor, Interfacial polymerization of thin film nanocomposite: A new concept for reverse osmosis membrane, J. Membr. Sci. 294 (2007) 1–7.
[19] G. Decher, Fuzzy nanoassemblies: Toward layered polymeric multicomposites, Science 277 (1997) 1232–1237.
[20] F. Caruso, R.A. Caruso, H. Mohwald, Nanoengineering of inorganic and hybrid hollow spheres by colloidal templating, Science 282 (1998) 1111–1114.
[21] S.S. Shiratori, M.F. Rubner, pH-dependent thickness behavior of sequentially adsorbed layers of weak polyelectrolytes, Macromolecules 33 (2000) 4213–4219.
[22] S.Y. Yang, M.F. Rubner, Micropatterning of polymer thin films with ph-sensitive and cross-linkable hydrogen-bonded polyelectrolyte multilayers, JACS 124 (2002) 2100–2101.
[23] Y. Li, R.A. VanHouten, A.E. Brink, J.E. Mcgrath, Purity characterization of 3,3′-disulfonated-4,4′-dichlorodiphenyl sulfone (SDCDPS) monomer by UV–vis spectroscopy, Polymer 49 (2008) 3014–3019.
[24] H.K. Jeong, Y.P. Lee, R.J.W.E. Lahaye, M.H. Park, K.H. An, I. J. Kim, C.W. Yang, C.Y. Park, R.S. Ruoff, Y.H. Lee, Evidence of Graphitic AB Stacking Order of Graphite Oxides, JACS 130 (2008) 1362–1366.